Pergamon

Solid State Communications, Vol. 108, No. 10, pp. 769–773, 1998

0038–1098/98 $ - see front matter

PII: S0038–1098(98)00430-X

COMBINATION OF SPECULAR AND OFF-SPECULAR LOW-ANGLE X-RAY DIFFRACTION IN THE STUDY OF METALLIC MULTILAYERS

A. de Bernabé,[a,b,*] M.J. Capitán,[b] H.E. Fischer,[c] C. Quirós,[d] C. Prieto,[a] J. Colino,[a] F. Mompeán[a] and J.M. Sanz[d]

[a]Instituto de Ciencia de Materiales de Madrid, Consejo Superior de Investigaciones Científicas, Cantoblanco, 28049-Madrid, Spain

[b]European Synchrotron Radiation Facility, B.P. 220, 38043-Grenoble, France

[c]Institut Max von Laue-Paul Langevin, B.P. 156, 38042-Grenoble, France

[d]Departamento de Física Aplicada (C-XII), Universidad Autónoma de Madrid, 28049-Madrid, Spain

(*Received* 13 *February* 1998; *in revised form* 20 *July* 1998; *accepted* 25 *August* 1998 *by J. Joffrin*)

The use of resonant low-angle X-ray diffraction, combining specular and off-specular scans, has been used to characterize accurately and self-consistently the mesoscopic structure and the quality of interfaces for a set of magnetron sputtered Co/Cu multilayers. In addition, the use of a simulation program to fit experimental patterns, which is based on the Distorted Wave Born Approximation has permitted to confirm its validity in the region of total external reflection in a system having a high degree of complexity. © 1998 Elsevier Science Ltd. All rights reserved

Keywords: A. magnetic films and multilayers, A. surfaces and interfaces, C. X-ray scattering.

1. INTRODUCTION

The explanation of physical properties of metallic multilayers (ML), such as giant magnetoresistance (GMR) [1], is directly related to the interfacial structure of these systems [2]. Therefore, a precise and reliable structural characterization becomes essential. The most widespread technique used to probe the structure of these materials is probably X-ray diffraction. For highly crystalline systems, high-angle X-ray diffraction is used to obtain a global measure of the sample's structure [2, 3] however, for polycrystalline samples the use of low-angle X-ray diffraction provides very useful results to the knowledge of the interfaces [4].

At low-angle X-ray diffraction, two kind of experiments can be performed: specular scans, which provide information about the dimension perpendicular to the surface of the multilayer (ML), allowing thus the determination of the layer thicknesses and root-mean-square (r.m.s.) roughness of the substrate (σ), interfaces and overlayer [5]; and off-specular scans (ω-rock or rocking curves and 2θ-rocks or detector scans) allow the reconstruction of the height–height correlation function of the roughness [6–8].

The most reliable way of obtaining information from reflectivity patterns consists of simulating reflectivity curves using a matricial calculation [5, 9–11]. Through this method, an accurate and self-consistent structural determination can be achieved when specular scans are completed by off-specular scans (ω-rock and 2θ-rock curves), which probe the in-plane structure of the ML and not simply the average electron density profile ($\rho(z)$) probed by specular scans. Such simulations are based on the Distorted Wave Born Approximation (DWBA) whose validity was reported in a previous work for near perfect semiconductor heterostructures in the Si/Ge system [8]. In that paper, Schlomka *et al*. studied the specular and off-specular scans of several samples with an increasing degree of complexity. The DWBA reproduced perfectly the off-specular scans taken at different wavevector transfer, in the region of total external reflection, for a Ge layer, a Ge/Si bilayer and finally a Ge/Si/Ge trilayer.

* Corresponding author.

In metallic multilayers, however, the growth mode is quite far from the epitaxial and quasiperfect obtained in semiconductor heterostructures. We have aimed then to prove the validity of the DWBA in a highly complex system, such as polycrystalline Co/Cu MLs. In addition, the combination of specular and off-specular scans has resulted in the obtention of a single set of self-consistent parameters which describe the mesoscopic structure of our system.

2. EXPERIMENTAL

Samples were grown on a Si (1 0 0) oxidized substrate using a DC-operated magnetron sputtering system with a residual pressure of 5×10^{-7} mbar. The Ar pressure used for deposition was 4.8×10^{-3} mbar at a constant substrate temperature of 60°C. The substrate was placed 8 cm away from magnetrons in order to get a good in-plane homogeneity of the sample. The deposition rates obtained were 2 nm/min for Co and 3 nm/min for Cu. Specially designed stainless steel screens were used to avoid mixing of Co and Cu during growth. The total sample thickness for the whole set was kept nearly constant around a value of 70 nm, for which the number of bilayers was varied; no buffer was used for growth. The samples grown, with a Co/Cu thickness ratio equal to unity, are represented as $[m\mathrm{Cu}/m\mathrm{Co}]_n$, where m is the layer thickness in Å and n the number of layers.

Experiments were carried out on the four circle goniometer setup at DCI D23-beamline (Laboratoire pour l'Utilization du Rayonnement Electromagnetique, Orsay, France) [12]. The beamline is equipped with a double crystal (Si(1 1 1)) monochromator with fixed exist and sagittal focusing. The experiments were performed 5 eV under the Co absorption K-edge, which was determined previously by recording the Near Edge X-ray Absorption Structure spectrum, to obtain the edge precisely. The detection was done combining an avalanche photodiode with a Ge(1 1 1) crystal analyzer tuned at the incident beam wavelength. The use of the analyzer permits to increase the angular resolution and the signal to background ratio by suppressing fluorescence. On the other hand, the avalanche photodiode has a good dynamic range (up to 50 000 counts/s). The instabilities of the incident beam were monitored through the diffuse scattering from a kapton film, recorded and corrected automatically in the data acquisition program. The experimental resolution function (a convolution of the slits used, beam divergence and the resolution of the detector) obtained from a rocking curve was 40 arcsec with an incident beam dimensions of 0.1×6 mm. A set of secondary slits placed just before the detector was set to 200 μm so as to get rid of diffuse scattering queues present in the ω-scans.

3. RESULTS AND DISCUSSION

Figure 1 shows the experimental reflectivity patterns obtained using synchrotron radiation, making use of the Co resonant dispersion for which the incident energy was selected to be 7704 eV. The hollow points represent the experimental data and lines are the mean square fits using the simulation program described ahead. Patterns correspond to four different samples with bilayer thicknesses ranging from 18 to 66 Å, in which the intensity position has been shifted in order to plot all of them together.

The small oscillations present in the spectra, correspond to sample-size oscillations (usually called Kiessig fringes). They arise from multiple interference between beams reflected at the top interface and at the multilayer–substrate interface. Superimposed to the Kiessig fringes, appear the multilayer peaks (they are Bragg-like peaks coming from the chemical modulation of the sample) which account for the periodicity of the ML. The number of Kiessig fringes between each pair of Bragg peaks is $2n-1$, ''n'' being the number of deposited bilayers. Finally, some long wavelength oscillation can be observed in some samples. Their nature is due to the uppermost Co layer which oxidizes and forms a thin oxide overlayer.

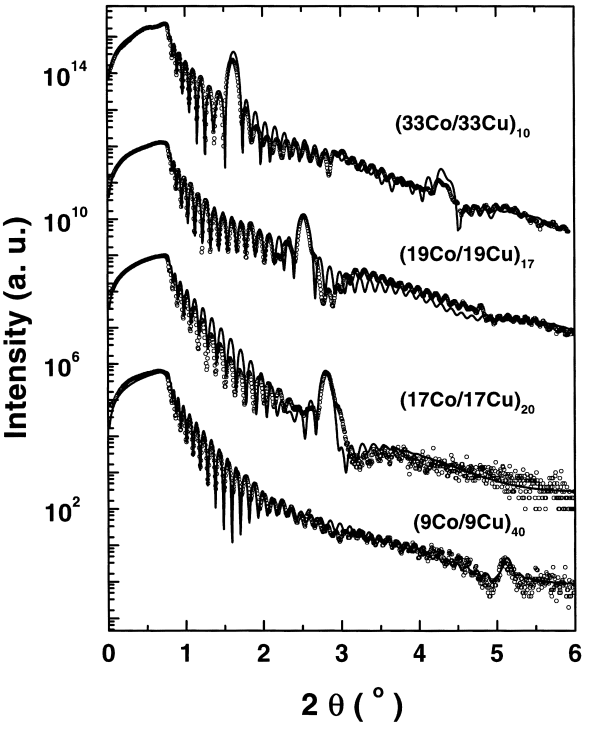

Fig. 1. Specular reflectivity patterns of Co/Cu multilayers recorded at an incident energy just under the Co absorption K-edge (7704 eV). Points correspond to the experimental patterns and solid lines have been calculated by the simulation program.

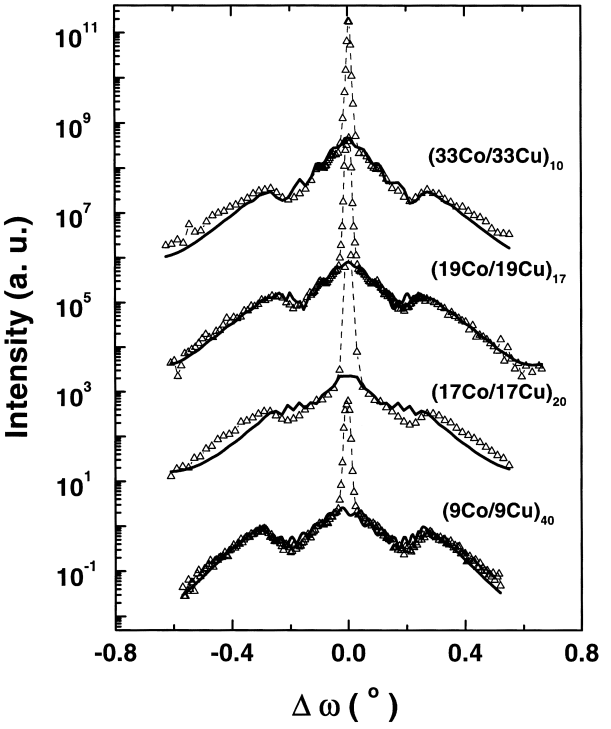

Fig. 2. Rocking curves taken at constant values of 2θ placed at a Kiessig maximum around $2\theta_M = 1.32°$. For the sake of clarity $\Delta\omega = \omega - \theta_M$ has been taken as the variable. The fits to the experimental patterns are based on the DWBA. The specular peak has not been reproduced in the simulations.

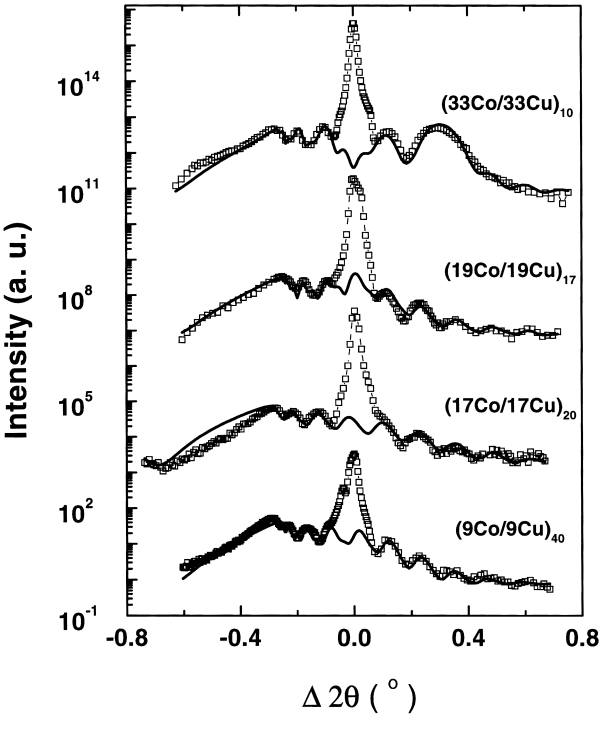

Fig. 3. 2θ-rock curves with their fit. The value of ω was held constant and around 0.66°. The variable used is $\Delta 2\theta = 2\theta - 2\theta_M$. For the simulations only the diffuse intensity has been taken into account.

Figure 2 shows the rocking curves corresponding to four samples. They have been taken at somehow different values of 2θ in order to be placed at a secondary (Kiessig) maximum in all of them and have an optimal contrast. They have been taken near the total reflection angle in order to see the dynamic effects in the MLs. Such effects are seen, in addition to the small oscillations near the central peak, through the so-called Yoneda wings [13] (which are broad maxima at both extrema of the plots after which the intensity drops sharply). They arise from interferences of the diffuse scattering by different interfaces and they are not reproducible within the Born Approximation. Spectrum $(17Co/17Cu)_{20}$ is the most inaccurate which may be due to a lower quality of the ML (something which matches well with the specular pattern), while the spectrum corresponding to $(19Co/19Cu)_{17}$ reproduces perfectly the structure and the Yoneda wings.

The last type of scans are the 2θ-rocks. They are done at a constant value of ω, which is half of the value of 2θ at which the rocking curves were taken. This scan geometry permits to see the reciprocal space in both the x and z directions. Figure 3 shows the spectra corresponding to the four samples from which ω-rocks were taken. In the spectrum corresponding to $(33Co/33Cu)_{10}$ sample there is an important increase in the oscillation at $2\theta = 1.6°$, this comes from an intensity leakage of the first Bragg peak of the multilayer, as can be seen from a glance at Fig. 3. In all the scans, the amplitude of the oscillations (related to vertical correlation length) as well as the intensity tendency (coming from the horizontal correlation length) are well reproduced, what permits to rely on the values of the correlation lengths (terms explained ahead in the section).

The simulations present in Figs 2 and 3 do not reproduce the central peak since only the diffuse scattering term has been considered in their calculation.

In order to obtain a quantitative and precise characterization of samples, measured patterns have been fitted using the following simulation program (a detailed description is in preparation [14]). For specular scans, the formalism given by Vidal and Vincent [10] has been used and the patterns have been fitted by a least square procedure. The Distorted Wave Born Approximation as presented by Daillant and Bélorgey [15] has been used for the off-specular simulations. The computer program, takes into account a great number of parameters which influence the reflectivity pattern obtained: layer thicknesses, roughnesses, deviations from the ideal cases (a linear and a Gaussian variation of the layer

thicknesses, a linear stretch of the roughnesses,…), as well as the roughness correlation lengths ξ_x and ξ_z and parameter h.

The electron densities and the absorption coefficients of the substrate, Co, Cu and the oxide layer, have been taken from the Sasaki tables [16]. Special attention has been paid to the oxide layer (thickness and roughness) since it became essential when trying to fit the experimental patterns. The fitting procedure was the following: once the parameters had been obtained from the specular patterns, they were used to simulate the off-specular scans in which only ξ_x, ξ_z, h and the roughnesses were varied. If the obtained fit is not satisfying, new roughness values are then introduced into the reflectivity simulations and varied to obtain a better fit. Again, those parameters were used to perform the off-specular simulations and the process repeated until a single set of roughness parameters was obtained. In the off-specular scans, the ξ_x obtained in the ω-rocks was used to simulate the 2θ-rocks and ξ_z was then varied until a good fit was reached.

To obtain the error bars, once the optimal fit had been reached by a root-mean-square process, the fit parameters were varied manually. When an appreciable change between the calculated and the experimental patterns had been observed, the difference was taken as the error bar.

Even if the specular reflectivity patterns provide very good and precise structural parameters of the system, when dealing with roughness, more than one possible solution may be obtained if diffuse scattering data are not accounted for. This observation, already stated in the literature [8], led us to perform off-specular scans in our samples to obtain a single solution for the roughnesses. In addition, they have permitted us to obtain the correlation lengths of the roughness profiles as well as the Hurst parameter, the combination of which permits to describe the morphology of the multilayer interfaces. The horizontal correlation length (ξ_x), represents approximately the distance between horizontal bumps. It allows to determine if there exists interdiffusion ($\xi_x < 15$ Å) or interface roughness ($\xi_x > 15$ Å). On the other hand, the vertical correlation length (ξ_z) gives an idea of the vertical distance throughout which the interfaces can be correlated. The Hurst parameter (h) ranges from 0 to 1 and gives an idea of the type of interface [17]. A value near zero will be characteristic of a jagged interface while a value near one is typical of flat and wide bumps in the interface.

The simulation results are summarized in Table 1. It should be remarked from these results that, while at a bilayer thickness (Λ) up to 38 Å the roughness of Co and Cu are equal, at a value of $\Lambda = 66$ Å there exists a difference in their roughness values, being lower for Cu. This is in agreement with the observed different growth behavior for Co and Cu. Co grows on Cu (1 1 1) forming islands up to a thickness of about 5 MLs after which it grows layer-by-layer [18]. Something interesting, as well, is the decreasing tendency of the oxide layer roughness as the oxide layer thickness increases. This behaviour, has been explained in a previous work and its reason attributed to the process of oxidation itself [19].

It seems worth at this point remarking on the validity of the Distorted Wave Born Approximation (DWBA), that it can perfectly reproduce the off-specular scans even in the region of total external reflection. The conclusions at which Schlomka *et al*. [8] arrived in their: Ge/Si/Ge system are now supported by these results in a system having structural complications such as a linear stretch of the roughness or a Gaussian distribution of the interlayer roughness. The DWBA is a very good approach to calculate the X-ray scattering cross section of rough interfaces near the critical angle.

4. CONCLUSIONS

The combination of specular and off-specular resonant X-ray diffraction experiments has permitted to obtain

Table 1. Values obtained by the fit procedure described in the text. From left to right, given values are: thickness of the Co layer, thickness of the Cu layer, Co r.m.s. roughness, Cu r.m.s. roughness, oxide layer thickness, oxide layer roughness, substrate roughness, horizontal correlation length, vertical correlation length and Hurst parameter

	d_{Co} (Å)	d_{Cu} (Å)	σ_{Co} (Å)	σ_{Cu} (Å)	d_O (Å)	σ_O (Å)	σ_S (Å)	ξ_x (Å)	ξ_z (Å)	h
$(9Co/9Cu)_{40}$	9.1	9.1	9	9	13	13.0	13	6000	700	0.45
	±0.1	±0.1	±1	±1	±1	±0.5	±2	±500	±200	
$(17Co/17Cu)_{20}$	17.1	17.0	12	12	18	8.0	12	5000	650	0.45
	±0.2	±0.2	±1	±1	±2	±0.5	±2	±2000	±100	
$(19Co/19Cu)_{17}$	19.1	19.1	8	8	50	3.0	8	8000	900	0.4
	±0.2	±0.2	±1	±1	±2	±0.2	±2	±2000	±100	
$(33Co/33Cu)_{10}$	33.0	33.0	12	6	33	4.5	10	8500	700	0.5
	±3	±0.3	±2	±2	±1	±0.5	±2	±500	±50	

accurately and self-consistently a single set of parameters describing the mesoscopic structure of magnetron-sputtering Co/Cu multilayers. In addition to describing the structure of these multilayers with such detail as a Gaussian distribution of the interface roughness, the Distorted Wave Born Approximation, used in the data treatment, has been proved to be perfectly valid to calculate the diffuse scattering cross section in a region within the total external reflection.

Acknowledgements—We gratefully acknowledge Prof. S. Lefebvre and Prof. M. Bessières from LURE for providing support for and during the experiments. One of us, AdB, wishes to thank E.S.R.F. for the stay which allowed us to perform this work. This work has been partially supported by the CICyT under contract no. MAT97/0725.

REFERENCES

1. Baibich, M.N., Broto, J.M., Fert, A., Nguyen Van Dan, F., Petroff, F., Eminent, P., Croquet, G., Friederich, A. and Chazelas, J., *Phys. Rev. Lett.*, **61,** 1988, 2472.
2. Fullerton, E.E., Kelly, D.M., Guimpel, J., Schuller, I.K. and Bruynseraede, Y., *Phys. Rev. Lett.*, **68,** 1992, 859.
3. De Santis, M., De Andrés, A., Raoux, D., Maurer, M., Ravet, M.F. and Piecuch, M., *Phys. Rev.*, **B46,** 1992, 15465.
4. Fischer, H.E., Fischer, H., Durand, O., Pellegrino, O., Andrieu, S., Piecuch, M., Lefebvre, S. and Bessière, M., *Nucl. Instrum. Methods*, **B97,** 1995, 402.
5. Chason, E. and Mayer, T., *Critical Review in Solid State and Materials Science*, **22,** 1997, 1.
6. Sinha, K., Sirota, E.B., Garoff, S. and Stanley, H.B., *Phys. Rev.*, **B38,** 1988, 229.
7. Holý, V. and Baumbach, T., *Phys. Rev.*, **B49,** 1994, 10668.
8. Schlomka, P., Tolan, M., Schwalowsky, L., Seeck, O.H., Stettner, J. and Press, W., *Phys. Rev.*, **B51,** 1992, 2311.
9. Parratt, L.G., *Phys. Rev.*, **95,** 1954, 359.
10. Vidal, B. and Vincent, P., *Appl. Optics*, **23,** 1984, 1794.
11. Lu, J.R., Lee, E.M. and Thomas, R.K., *Acta. Cryst.*, **A52,** 1996, 11.
12. Elkaim, E., Lefebvre, S., Kahn, R., Berar, J.F., Lemonnier, M. and Bessière, M., *Rev. Sci. Instrum.*, **63,** 1992, 988.
13. Yoneda, Y., *Phys. Rev.*, **131,** 1963, 2010.
14. Fischer, H.E., Fisher, H. and Piecuch, M. (unpublished).
15. Daillant, J. and Bélorgey, O., *J. Chem. Phys.*, **97,** 1992, 5824.
16. *Sasaki Tables*, National Laboratory for High Energy Physics, Japan.
17. Mandelbrot, B.B., *The Fractal Geometry of Nature*. Freeman, New York, 1982.
18. de la Figuera, J., Prieto, J.E., Ocal, C. and Miranda, R., *Phys. Rev.*, **B47,** 1993, 13 043.
19. de Bernabé, A., Capitán, M.J., Fischer, H.E., Lequien, S., Prieto, C., Colino, J., Mompeán, F., Lefebvre, S., Bessiere, M., Quirós, C. and Sanz, J.M., *Vacuum* (in press).